RSC Advances

PAPER

View Article Online
View Journal | View Issue



Cite this: *RSC Adv.*, 2021, **11**, 9366

# Copper based on diaminonaphthalene-coated magnetic nanoparticles as robust catalysts for catalytic oxidation reactions and C–S cross-coupling reactions†

Nasrin Yarmohammadi, Mohammad Ghadermazi* and Roya Mozafari

Received 7th February 2021
Accepted 15th February 2021

DOI: 10.1039/d1ra01029h

rsc.li/rsc-advances

In this work, the immobilization of copper(II) on the surface of 1,8-diaminonaphthalene (DAN)-coated magnetic nanoparticles provides a highly active catalyst for the oxidation reaction of sulfides to sulfoxides and the oxidative coupling of thiols to disulfides using hydrogen peroxide ($H_2O_2$). This catalyst was also applied for the one-pot synthesis of symmetrical sulfides *via* the reaction of aryl halides with thiourea as the sulfur source in the presence of NaOH instead of former strongly basic and harsh reaction conditions. Under optimum conditions, the synthesis yields of sulfoxides, symmetrical sulfides, and disulfides were about 99%, 95%, and 96% respectively with highest selectivity. The heterogeneous copper-based catalyst has advantages such as the easy recyclability of the catalyst, the easy separation of the product and the less wastage of products during the separation of the catalyst. This heterogeneous nanocatalyst was characterized by FESEM, FT-IR, VSM, XRD, EDX, ICP and TGA. Furthermore, the recycled catalyst can be reused for several runs and is economically effective.



## 1. Introduction

Catalysis is the master key to chemical transformations.[1] Almost all biological reactions and more than 90% of industrial processes need catalysts.[2] It is known that homogeneous catalysts, because of the solubility in the reaction medium, have good performance.[3–5] However, these materials have disadvantages such as the generation of highly toxic wastes[6] and time-consuming catalyst separation.[7] Additionally, metal catalysts are recycled with difficulty, and they produce high amounts of wastes. In industrial applications, homogeneous catalysts in comparison with heterogeneous catalysts have a contribution of less than 20%.[3] From the standpoint of green chemistry, using heterogeneous catalysts to run procedures for making fine chemical products has attracted remarkable attention from industrial and academic researchers. However, the catalytic activity of heterogeneous catalysts is reduced over time.[2,8,9] Magnetic nanoparticle (MNP) catalysts can address the recovery and separation problems encountered in many catalytic reactions. Furthermore, these catalysts show not only high catalytic activity, but also a high degree of chemical stability. MNP catalysts can be recycled with an external magnetic field.[10–13]

DAN has been widely utilized in the structure of inorganic and organometallic complexes as a suitable ligand because of having bidentate nucleophilic centers. This ligand has a unique structure and properties that make it an interesting choice for a diverse range of applications over recent years. DAN complex has been used in various fields such as optical devices, biological applications, conducting polymers,[14] sensors, and electronic science.[15] This ligand has been recently considered because of its unique properties in heterocyclic synthesis.[16]

Noble metals such as Pt, Cu, Au and Rh have been incorporated into the structure of nanoparticles.[17–21] Among the mentioned metals, copper nanoparticles have been paid attention due to their catalytic activity, suitable treating costs, and high conductivity, which make them useful in nanoscience.[22–24] Cu-based materials, because of the several oxidation states of this metal, can catalyze many oxidative reactions *via* both one- and two-electron pathways. The feasible modification of the properties of these materials *via* different synthetic policies and post-synthetic chemical treatments has engendered considerable interest in the field of catalysis. Furthermore, Cu's high boiling point makes it a good candidate for reactions under hard conditions such as high temperature and pressure.[25]

It is clear that sulfides are significant precursors for the synthesis of sulfoxides. Sulfoxides have been reported to possess widespread pharmaceutical functions and biological properties such as anticancer, antifungal and anti-atherosclerotic activities.[26,27] Furthermore, they have been

*Department of Chemistry, University of Kurdistan, P.O. Box 66135-416, Sanandaj, Iran. E-mail: mghadermazi@yahoo.com; Fax: +98 87 3324133; Tel: +98 87 33624133*

† Electronic supplementary information (ESI) available. See DOI: 10.1039/d1ra01029h

extensively utilized for the preparation of carbon–carbon bond and rearrangement reactions.[28,29]

Moreover, disulfides have important applications in biological and industrial fields such as protecting agents[25] stabilization of protein structures,[30] and vulcanizing entities.[31,32] The catalytic formation of the C–S bond is a basic transformation in synthetic reactions. Their importance is based on the application in pharmaceutical industries and preparing a scaffold for aryl sulfides as intermediates in synthetic organic chemistry.[33,34] Although the sulfide and disulfide oxidation reactions have been studied extensively,[35–44] it is necessary to introduce procedures that are more simple, efficient and selective. Herein, a magnetically separable heterogeneous catalyst was fabricated by anchoring a Cu complex supported on functionalized $CoFe_2O_4$ nanoparticles. This catalyst exhibits efficient oxidation reactions of sulfides to sulfoxides and oxidative coupling of thiols to disulfides utilizing hydrogen peroxide. It is necessary to introduce procedures that are more simple, efficient and selective. Moreover, we used the prepared nanoparticle as a catalyst for the odorless C–S cross-coupling reaction of aryl halides under mild conditions. Furthermore, the catalyst is separated from the reaction media *via* magnetic decantation and the nanocatalyst can be recycled several times.

## 2. Experimental

### 2.1 Materials and methods

Chemical materials were supplied from Sigma-Aldrich and Merck and used as received. The X-ray powder diffraction (XRD) data of the $CoFe_2O_4$-DAN-Cu(II) nanocatalyst were obtained using a Co radiation source with a wavelength of $\lambda = 1.78897$ Å, 40 kV. The morphology of the nanocatalyst was investigated by FESEM-TESCAN MIRA3, operating at a voltage of 30 kV, which was gold-coated using a sputtering coater. FT-IR spectra of the prepared samples were recorded from a KBr disc using a VRTEX 70 model BRUKER FT-IR spectrophotometer, in the range of 400 and 4000 $cm^{-1}$. $^1H$ NMR spectra were recorded using a Bruker 400 MHz NMR AVANCE 300 spectrometer. TGA was performed using a Shimadzu DTG-60 instrument in the temperature range 25–800 °C. Energy-dispersive X-ray spectroscopy (EDX) was used for the elemental analysis. The copper content in the catalyst was evaluated by inductively coupled plasma-optical emission spectrometry (ICP-OES; 730-ES Varian). TEM analysis of the catalyst was performed using a Zeiss-EM10C transmission electron microscope.

### 2.2 Preparation of $CoFe_2O_4$-DAN-Cu(II) nanocatalysts

First, the mixture of $Fe(NO_3)_3 \cdot 6H_2O$ (16 mmol, 5.584 g) and $CO(NO_3)_2 \cdot 6H_2O$ (8 mmol, 2.328 g) was dissolved in deionized water (20 mL) under vigorous stirring conditions until the components were dissolved. A brown precipitate was produced by adding sodium hydroxide (15 mL, 3 M) under magnetic stirring. After adjusting the pH to 11, the solution was heated at 80 °C for an hour. The obtained black magnetic nanoparticles were separated, washed five times with distilled water/ethanol mixture solution, and dried in an oven at 60 °C for 14 h. To prepare $CoFe_2O_4$–Cl, 1 g of MNP powder was dispersed in 50 mL of toluene under sonication for 30 min, then (1 mL) of 3-chloropropyltrimethoxysilane (CPTMS) was added to the reaction mixture and refluxed for 24 h. The obtained nanoparticles were separated by an external magnet, washed with ethanol/water mixture solution and dried in an oven at 80 °C. For the functionalization of $CoFe_2O_4$–Cl with 1,8-diaminonaphthalene, 1 g of the suspension of $CoFe_2O_4$–Cl in 70 mL of acetonitrile was added to a mixture of KI (6 mmol, 0.996 g) and $K_2CO_3$ (6 mmol, 0.828 g). The obtained mixture was stirred magnetically at room

Table 1 Optimization of conditions for oxidation of sulfides to sulfoxides in the presence of $CoFe_2O_4$-DAN-Cu(II)

| Entry | Catalyst (mg) | Oxidation agent | Solvent | Temp. (°C) | Time (min) | Yield[a] (%) |
|---|---|---|---|---|---|---|
| 1 | 25 | $H_2O_2$ (0.5 mL) | Acetonitrile | 25 | 20 | 85 |
| 2 | 25 | $H_2O_2$ (0.5 mL) | *n*-Hexane | 25 | 120 | 25 |
| 3 | 25 | $H_2O_2$ (0.5 mL) | EtOAc | 25 | 25 | 80 |
| 4 | 25 | $H_2O_2$ (0.5 mL) | $H_2O$ | 25 | 30 | 75 |
| 5 | 25 | $H_2O_2$ (0.5 mL) | Ethanol | 25 | 15 | 99 |
| 6 | — | $H_2O_2$ (0.5 mL) | Ethanol | 25 | 140 | Trace |
| 7 | 25 | $H_2O_2$ (0.55 mL) | Ethanol | 25 | 15 | 98 |
| 8 | 25 | $H_2O_2$ (0.4 mL) | Ethanol | 25 | 25 | 85 |
| 9 | 25 | $H_2O_2$ (0.3 mL) | Ethanol | 25 | 25 | 79 |
| 10 | 25 | $H_2O_2$ (0.2 mL) | Ethanol | 25 | 25 | 68 |
| 11 | 25 | $H_2O_2$ (0.1 mL) | Ethanol | 25 | 25 | 43 |
| 12 | 25 | — | Ethanol | 25 | 140 | Trace |
| 13 | 7 | $H_2O_2$ (0.5 mL) | Ethanol | 25 | 25 | 55 |
| 14 | 9 | $H_2O_2$ (0.5 mL) | Ethanol | 25 | 25 | 68 |
| 15 | 10 | $H_2O_2$ (0.5 mL) | Ethanol | 25 | 25 | 85 |
| 16 | $CuCl_2 \cdot 2H_2O$ | $H_2O_2$ (0.5 mL) | Ethanol | 25 | 65 | 40 |
| 17 | 25 | $NaIO_4$ (2 mmol) | $CH_3CN/H_2O$ | 25 | 100 | 85 |
| 18 | 25 | Oxone (0.3689 g, 0.6 mmol) | Ethanol | 60 | 720 | 90 |
| 19 | 25 | $O_2$ (2 MPa) | PEG | 100 | 720 | 10 |

[a] Isolated yields.

temperature for 35 min. Afterwards, 1,8-diaminonaphthalene (18 mmol, 2.84 g) was added to the solution and the mixture was refluxed for 24 h. The resulting mixture was then filtered, washed with 95% ethanol and dried at 60 °C to obtain $CoFe_2O_4$-DAN. Finally, the $CoFe_2O_4$-DAN-Cu(II) nanoparticles were afforded by mixing $CoFe_2O_4$-DAN (2 g) and $CuCl_2 \cdot 2H_2O$ (1 g) in 20 mL of ethanol and stirring under reflux for 18 h. The obtained product was then magnetically separated, washed with ethanol and dried at 50 °C.

### 2.3 General procedure for oxidation of sulfides to sulfoxides with $H_2O_2$ in the presence of $CoFe_2O_4$-DAN-Cu(II)

In a 25 mL round-bottom flask equipped with a magnetic stirrer and heater, a suspension of 1 mmol sulfide and 0.025 g catalyst in ethanol (3 mL) was stirred for 2 min at room temperature. Then, $H_2O_2$ (0.5 mL, 4.90 mmol) was added dropwise to the reaction mixture and the obtained blend was stirred at 25 °C for appropriate time (Table 1). After reaction completion, ethyl acetate (2 × 5 mL) was added to the mixture, a heterogeneous catalyst was separated from the mixture using an external magnet. After that, the filtered solution was dried over $Na_2SO_4$ (2 g). The products were obtained by evaporating the organic solvent.

### 2.4 Typical procedure for the synthesis of derivative sulfides in the presence of $CoFe_2O_4$-DAN-Cu(II)

In a 25 mL round-bottom flask equipped with a magnetic stirrer and heater, a mixture of the aryl halide (1 mmol), thiourea (1 mmol, 0.076 g), NaOH (1 mmol, 0.04 g), and $CoFe_2O_4$-DAN-Cu(II) (0.03 g) nanocatalyst were mixed under stirring at 130 °C in 3 mL DMSO for an appropriate time specified in Table 2. After reaction completion (monitored by TLC), $CH_2Cl_2$ was added to the reaction mixture, the heterogeneous catalyst was magnetically decanted. The filtered solution was washed with $H_2O$ and dehydrated over $Na_2SO_4$. After organic solvent volatilization, the corresponding sulfide was obtained.

### 2.5 Typical procedure for oxidative coupling of thiols to disulfides with $H_2O_2$ in the presence of $CoFe_2O_4$-DAN-Cu(II)

In a typical experiment, thiol (1 mmol), $CoFe_2O_4$-DAN-Cu(II) (0.025 g) and ethanol (3 mL) were taken in a 25 mL round-bottom flask, equipped with a magnetic stirrer and heater.

Table 2 Oxidation of sulfides with $CoFe_2O_4$-DAN-Cu(II) in the presence of $H_2O_2$[a]

| Entry | Substrate | Product | Time (min) | Yield[b] (%) | Mp (°C) |
|---|---|---|---|---|---|
| 1 | 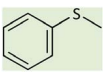 |  | 15 | 99 | Oil[51] |
| 2 |  |  | 15 | 95 | Oil[52] |
| 3 |  | 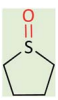 | 2 | 93 | Oil[53] |
| 4 | 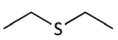 | 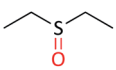 | 27 | 95 | Oil[54] |
| 5 | 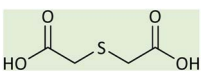 | 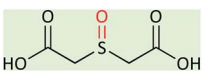 | 6 | 94 | Oil[53] |
| 6 | 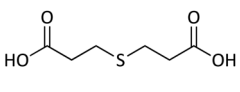 | 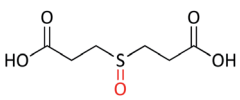 | 20 | 93 | 112–114 (ref. 11) |
| 7 | 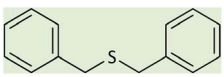 | 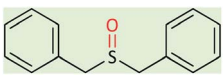 | 85 | 88 | 130–133 (ref. 55) |
| 8 | 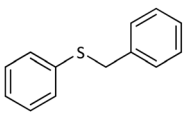 | 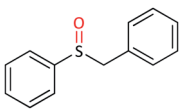 | 100 | 87 | 117–119 (ref. 55) |
| 9 | 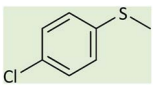 | 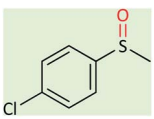 | 105 | 85 | Oil[47] |

[a] Reaction conditions: catalyst (0.025 g), sulfide (1 mmol), 30% $H_2O_2$ (0.5 mL) and solvent (3 mL) at 25 °C. [b] Isolated yields.

Table 3 Optimization of conditions for sulfide synthesis in the presence of $CoFe_2O_4$-DAN-Cu(II)

| Entry | Catalyst (mg) | Base | Thiourea (mmol) | Solvent | Temp. (°C) | Time (h) | Yield[a] (%) |
|---|---|---|---|---|---|---|---|
| 1 | 30 | NaOH | 1 | $H_2O$ | 130 | 4 | N.R. |
| 2 | 30 | NaOH | 1 | PEG | 130 | 4 | N.R. |
| 3 | 30 | NaOH | 1 | DMF | 130 | 3.5 | 52 |
| 4 | 30 | NaOH | 1 | DMSO | 130 | 2.5 | 95 |
| 5 | 30 | NaOH | 1 | Toluene | 130 | 3 | 35 |
| 6 | — | NaOH | 1 | DMSO | 130 | 5 | Trace |
| 7 | 30 | NaOH | 0.5 | DMSO | 130 | 3.5 | 67 |
| 8 | 30 | NaOH | 0.8 | DMSO | 130 | 3.5 | 82 |
| 9 | 8 | NaOH | 1 | DMSO | 130 | 3.5 | 37 |
| 10 | 10 | NaOH | 1 | DMSO | 130 | 3.5 | 52 |
| 11 | 20 | NaOH | 1 | DMSO | 130 | 3.5 | 79 |
| 12 | 30 | NaOH | 1 | DMSO | 45 | 3.5 | 40 |
| 13 | 30 | NaOH | 1 | DMSO | 65 | 3.5 | 65 |
| 14 | 30 | NaOH | 1 | DMSO | 85 | 3.5 | 75 |
| 15 | 30 | NaOH | 1 | DMSO | 100 | 3.5 | 85 |
| 16 | 30 | KOH | 1 | DMSO | 130 | 3.5 | Trace |
| 17 | 30 | $Na_2CO_3$ | 1 | DMSO | 130 | 3.5 | Trace |
| 18 | $CuCl_2 \cdot 2H_2O$ | NaOH | 1 | DMSO | 130 | 4 | Trace |

[a] Isolated yields.

The solution was stirred for 2 min at room temperature. After that, $H_2O_2$ (0.4 mL, 3.92 mmol) was added dropwise to the reaction mixture and the obtained blend was stirred at 25 °C for an appropriate time (Table 3). The reaction process was monitored by TLC (ethyl acetate/*n*-hexane: 1 : 4). Upon completion of the reaction, the nanocatalyst was magnetically isolated and the product was extracted with ethyl acetate. The product was obtained, dried over anhydrous $Na_2SO_4$ and evaporated to yield pure products.

### 2.6 Selected spectral data

**2.6.1 Methyl phenyl sulfoxide.** $^1$H-NMR (300 MHz, $CDCl_3$, ppm): $\delta$ 2.98 (s, 3H), 7.46–7.87 (m, 5H); $^{13}$C-NMR (75 MHz, $CDCl_3$, ppm): $\delta$ 44.15, 124.44, 129.60, 131.45, 144.29. IR (KBr) ($cm^{-1}$): $\nu$ (S=O): 1079.

**2.6.2 Benzyl phenyl sulfoxide.** $^1$H-NMR (400 MHz, DMSO, ppm): $\delta$ 4.68 (s, 2H), 7.14–7.34 (m, 4H), 7.53–7.75 (m, 4H). $^{13}$C-NMR (75 MHz, DMSO, ppm): $\delta$ 61.15, 128.51–128.81, 129.16, 129.60–131.45, 138.83. IR (KBr) ($cm^{-1}$): $\nu$ (S=O): 1068.

**2.6.3 Dibenzyl sulfoxide.** $^1$H-NMR (400 MHz, DMSO, ppm): $\delta$ 4.16 (S, 4H), 7.29–7.45 (m, 10H); $^{13}$C-NMR (75 MHz, DMSO, ppm): $\delta$ 58.03, 127.57, 129.03, 130.18, 130.91. IR (KBr) ($cm^{-1}$): $\nu$ (S=O): 1026–1089.

**2.6.4 Diphenyl sulfide.** $^1$H-NMR (400 MHz, DMSO, ppm): $\delta$ 7.72–7.32 (m, 4H), 7.32–7.38 (m, 4H); $^{13}$C-NMR (75 MHz, $CDCl_3$, ppm): $\delta$ 127.51, 129.66, 131.01, 134. 83. IR (KBr) ($cm^{-1}$): 3421, 3080, 1592, 1333, 1108, 1104, 838, 631.

**2.6.5 Chemical 4,4′-thiodiphenol.** $^1$H-NMR (400 MHz, $CDCl_3$, ppm): $\delta$ 6.63–6.68 (m, 4H), 7.713–7.732 (m, 4H); $^{13}$C-NMR (75 MHz, $CDCl_3$, ppm): $\delta$ 123.64, 128.81, 158.83. IR (KBr) ($cm^{-1}$): 3421, 2822, 1625, 1498, 1117, 933, 797, 501.

**2.6.6 Di-*p*-tolylsulfane.** $^1$H-NMR (400 MHz, DMSO, ppm): $\delta$ 2.43 (s, 6H), 7.26–7.32 (m, 4H), 7.33–7.49 (m, 4H); $^{13}$C-NMR (400 MHz, $CDCl_3$, ppm): $\delta$ 22.15, 131.46, 131.69, 132. 83, 139.16. IR (KBr) ($cm^{-1}$): 3333, 2854, 1625, 1425, 1303, 1073, 838, 697.

**2.6.7 Dibenzylsulfane.** $^1$H-NMR (300 MHz, DMSO, ppm): $\delta$ 3. 377 (s, 4H), 7.261–7.412 (m, 4H); $^{13}$C-NMR (100 MHz, DMSO, ppm): $\delta$ 35.15, 127.165, 128.69, 138.16. IR (KBr) ($cm^{-1}$): $\nu$ (S–S): 1069.

### 2.7 Procedure for the recovery of the $CoFe_2O_4$-DAN-Cu(II) nanocatalyst

For recycling of the catalyst in the mentioned reactions, methyl phenyl sulfide, iodobenzene, and 4-methylthiophenol as model substrates were used under optimized conditions. After completion of the reaction, the $CoFe_2O_4$-DAN-Cu(II) nanocatalyst was separated from the reaction mixture by a magnet, washed, and dried at 80 C. The obtained nanocatalyst was used for the next reaction under optimum conditions. This procedure was repeated for nine runs. Selected spectral data using $^1$H-NMR spectra for sulfoxides, symmetrical sulfides, and disulfides are given in the ESI.†

## 3. Results and discussions

$CoFe_2O_4$-DAN-Cu(II) nanoparticles were synthesized according to a three-step procedure (Scheme 1). Cobalt ferrite was prepared by the co-precipitation of aqueous $Fe^{3+}$ and $Co^{2+}$ salt solutions in the presence of a base at 80 °C.[45] The functionalization of the hydroxyl groups of $CoFe_2O_4$ with CPTMS yielded $CoFe_2O_4$–Cl. Finally, $CoFe_2O_4$-DAN was treated with $CuCl_2 \cdot 2H_2O$ to give $CoFe_2O_4$-DAN-Cu(II) *via* an electrostatic interaction between copper ions and functional groups of $CoFe_2O_4$-DAN. The catalytic performance of the synthesized heterogeneous nanocatalyst was evaluated in the oxidation of sulfides, thiols and C–S cross-coupling reactions of aryl halides (Scheme 1).

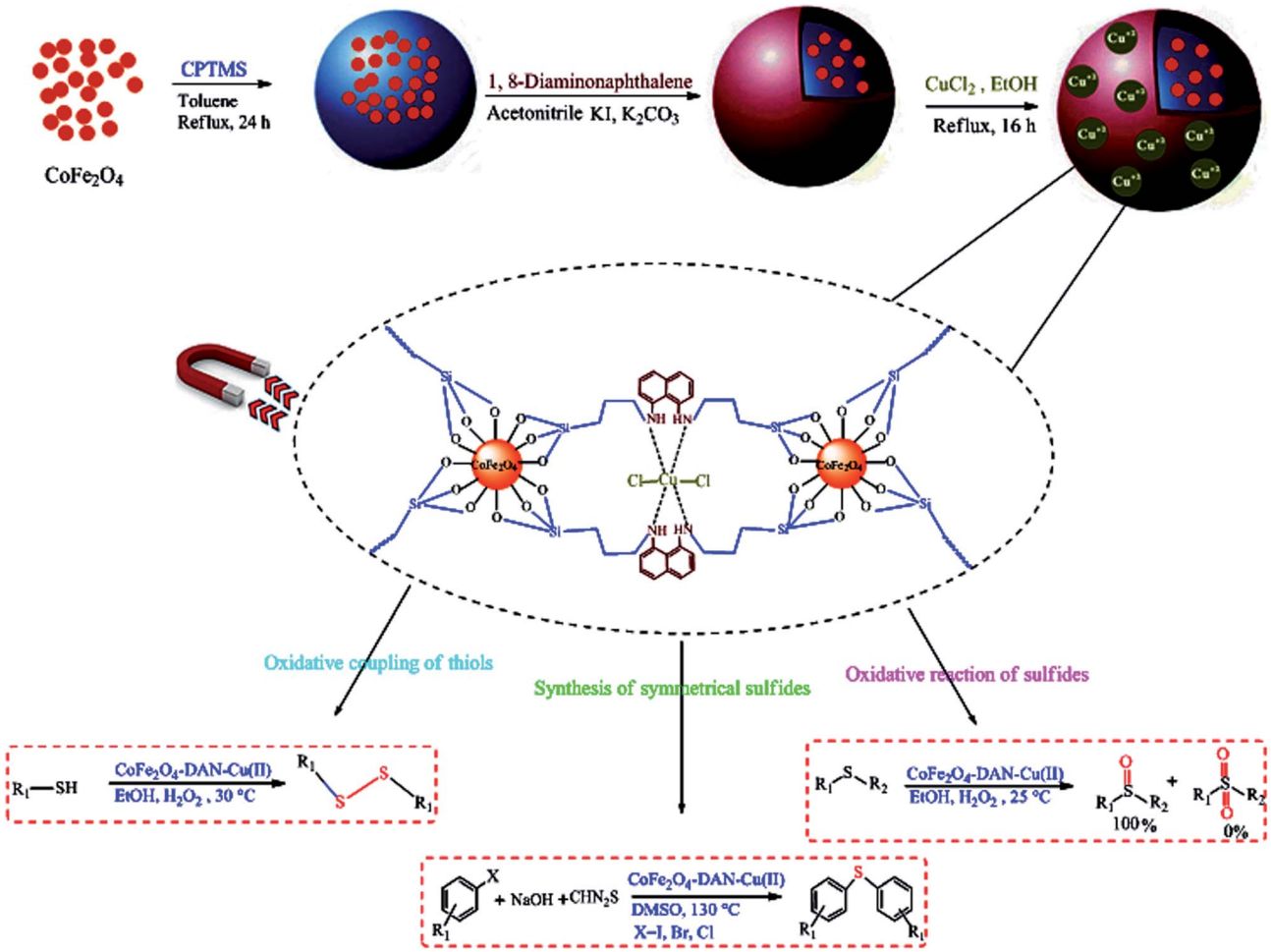


Scheme 1 Preparation of $CoFe_2O_4$-DAN-Cu(II) nanocatalyst and its application in the oxidation of sulfides, thiols and C–S cross-coupling reactions.

### 3.1 Catalyst characterization

The obtained $CoFe_2O_4$-DAN-Cu(II) nanocatalyst was characterized by FESEM, FT-IR, EDX, TGA, VSM, XRD and ICP-OES analysis. Fig. 1 depicts the particle shape and surface morphology of $CoFe_2O_4$ and $CoFe_2O_4$-DAN-Cu(II). According to the SEM images, prepared nanoparticles were made up of homogeneous and quite spherical particles ranging about 21 nm in size. Moreover, grafting copper complex onto nanoparticles did not cause any significant change in the morphology and structure of $CoFe_2O_4$-DAN-Cu(II) nanoparticles. Transmission electron microscopic (TEM) study of the $CoFe_2O_4$-DAN-Cu(II) nanocatalyst is also shown in Fig. 1d. This image shows that $CoFe_2O_4$ was encapsulated by copper complexes, and the particles show an average diameter of about 21 nm, like the sizes resulting from the SEM measurements.

The EDX spectrum can provide qualitative information about the types of different chemical elements in the catalyst. Fig. S1† shows an EDX spectrum of $CoFe_2O_4$-DAN-Cu(II) and Fe, Si, N, C, O, and Cu were detected. On the basis of these results, it is demonstrated that copper(II) was immobilized on the surface of diaminonaphthalene-coated MNPs. Moreover, the elemental mapping images indicate the uniform dispersion of copper in the nanocatalyst. This has been further confirmed from the EDX spectrum of the nanocatalyst. The ICP-OES technique was studied for the measurement of Cu amounts loaded onto the modified surface of the nanoparticles, from which the exact amount was found to be 0.43 mmol $g^{-1}$.

The magnetic properties of bare $CoFe_2O_4$ (a) and $CoFe_2O_4$-DAN-Cu(II) (b) were studied using a vibrating sample magnetometer (VSM) with a peak field of 15 kOe (Fig. 2). The saturation magnetization value ($M_s$) of these nanoparticles was found to be 53.7 and 36.6 emu $g^{-1}$ respectively. As seen, the magnetization of the synthesized nanocatalyst is decreased because of the copper complex coated on $CoFe_2O_4$ MNPs; however, this reduction is insignificant for the separation of this nanocatalyst using an external magnetic field.

Fig. S2† shows the thermogravimetric analysis (TGA) curve of $CoFe_2O_4$-DAN-Cu(II) at a temperature ranging from 25 °C to 800 °C. The first weight loss was about 2 wt%, until the temperature of 150 °C, which is attributed to the removal of adsorbed solvents and surface hydroxyl groups.[47] In the range of 200–500 °C, decomposition of the organic layer and Cu complex grafted onto the surface of magnetite nanoparticles was shown.

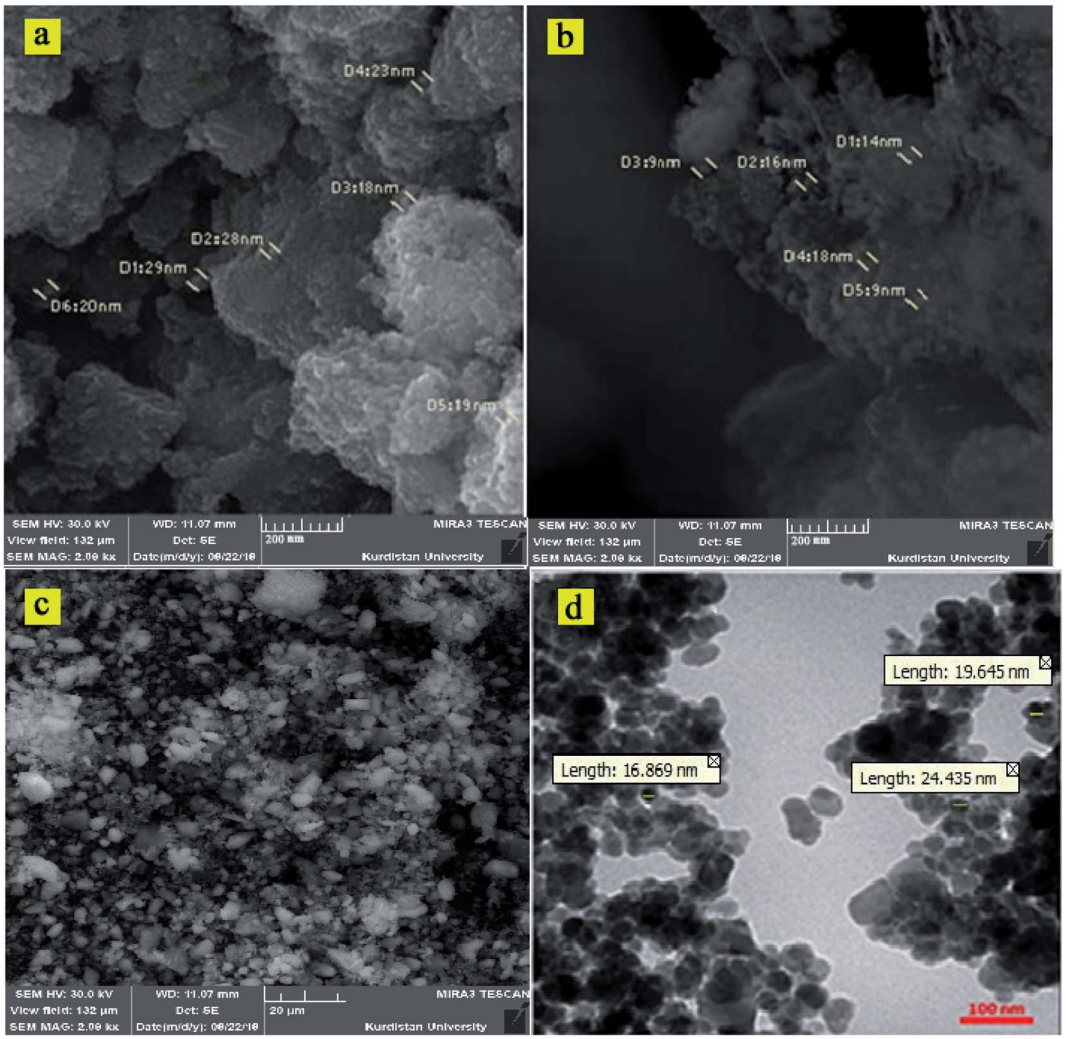


Fig. 1 SEM images of $CoFe_2O_4$ at (a) 200 nm and $CoFe_2O_4$-DAN-Cu(II) at (b) 200 nm, (c) 20 μm, and TEM image of $CoFe_2O_4$-DAN-Cu(II) (d).

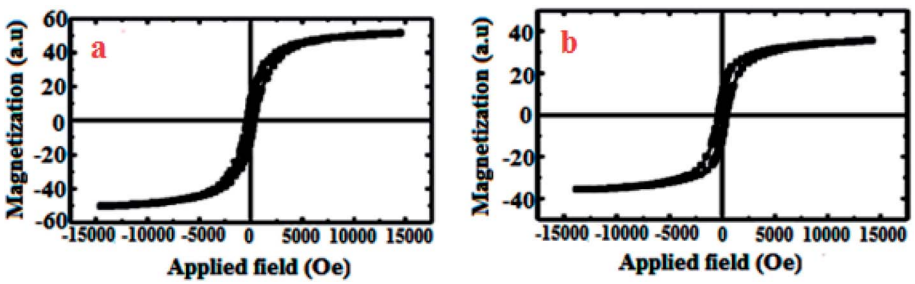


Fig. 2 VSM curves of $CoFe_2O_4$ (a) and $CoFe_2O_4$-DAN-Cu(II) nanocatalyst (b).

On the basis of these results, $CoFe_2O_4$-DAN-Cu(II) has high thermal stability that spreads its application for several types of organic reactions.

The FT-IR spectra shown in Fig. S3† exhibit a comparison of bare $CoFe_2O_4$, $CoFe_2O_4Cl$, $CoFe_2O_4$-DAN and $CoFe_2O_4$-DAN-Cu(II) nanoparticles. The pure nanoparticles exhibit bands at 430 and 586 $cm^{-1}$ characteristic of the Fe–O stretching vibration in the tetrahedral and octahedral sites of the $CoFe_2O_4$, respectively. The broad band at 3403 $cm^{-1}$ can be related to characteristic –OH bands of $CoFe_2O_4$ (Fig. S3a†).[48] The band located at 2986 $cm^{-1}$ in the spectrum of $CoFe_2O_4$–Cl could be attributed to the stretching vibration of C–H (Fig. S3b†). The sharp peak at 1101 $cm^{-1}$ is attributed to the Si–O stretching vibration, and these bands are assigned to the characteristic absorptions of the linker CPTMS attached on the cobalt ferrite surface (Fig. S3b†).[49] The peaks at about 1440–1660 $cm^{-1}$ are

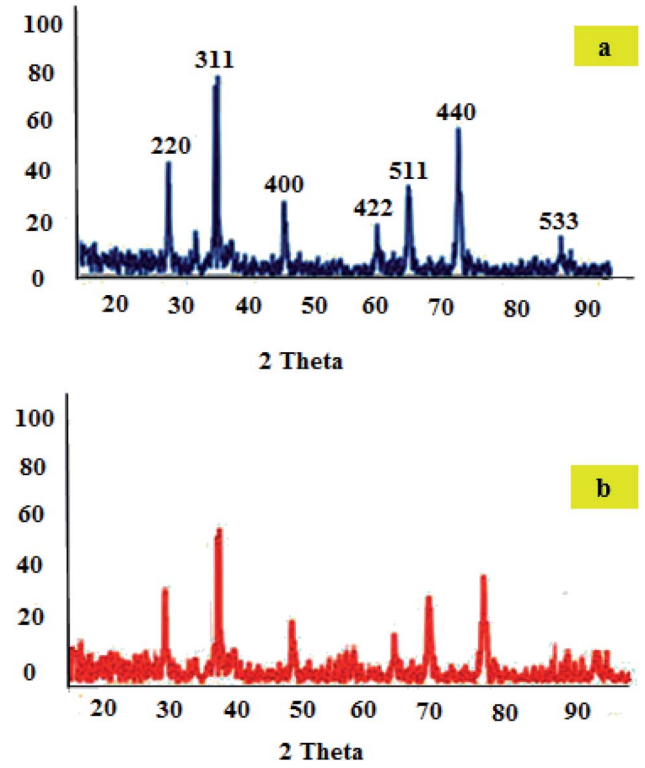


Fig. 3 XRD patterns of $CoFe_2O_4$ (a) and $CoFe_2O_4$-DAN-Cu(II) (b) nanocatalysts.

due to the amine group bending vibration of the 1,8-diaminonaphthalene ring and also the band at 3400 $cm^{-1}$ is assigned to the amine stretching band of the synthesized nanoparticles (Fig. S3c†).[50] In the spectrum of $CoFe_2O_4$-DAN-Cu(II), however, the shift absorption of amine to a lower wave number occurs, which is attributed to a robust interaction between the N group of the copper complex on $CoFe_2O_4$ (Fig. S3d†).

Fig. 3 represents the XRD patterns of $CoFe_2O_4$ and $CoFe_2O_4$-DAN-Cu(II). The diffraction peaks related to Bragg's reflections from the (2 2 0), (3 1 1), (4 0 0), (4 2 2), (5 1 1), (4 4 0), and (5 3 3) planes correspond to the standard spinel structure of $CoFe_2O_4$ (JCPDS 02-8517) (Fig. 3a).[46] Furthermore, on the basis of the Debye–Scherrer equation, the crystallite size of $CoFe_2O_4$ was about 21 nm. The XRD pattern of $CoFe_2O_4$-DAN-Cu(II) exhibits characteristic peaks whose relative intensities match well with the standard XRD data of $CoFe_2O_4$. These results indicate that the spinel structure of the $CoFe_2O_4$ framework was well maintained during the process of catalyst preparation.

### 3.2 Catalytic activity

After synthesis and characterization of the nanocatalyst, we decided to study the catalytic activity in the oxidation of sulfides. Therefore, for optimizing the reaction conditions for the oxidation of sulfides, methyl phenyl sulfide was used as a model substrate and different amounts of the catalyst, $H_2O_2$ and various solvents were studied. The results are summed up in Table 1. In order to obtain the optimum solvents of the reaction, the oxidation reaction was performed in different solvents. It was observed that polar aprotic solvents such as acetonitrile, ethyl acetate, water and ethanol obtained 85%, 80%, 75% and 99% conversion of sulfide respectively (Table 1, entries 1 and 3–5). Moreover, the reaction was performed in non-polar solvents like *n*-hexane that gave only 25% yield (Table 1, entry 2). These results indicated that ethanol is the appropriate solvent for this reaction. Moreover, it is seen that selectivity remained the same in all solvents and sulfoxide is the only product of this system. Then, different oxidation agents such as $NaIO_4$, oxone ($2KHSO_5 \cdot KHSO_4 \cdot K_2SO_4$) and $O_2$ were studied (Table 1, entries 17–19). The oxidant $H_2O_2$ showed higher activity than other used oxidants, while the sulfoxide selectivity was kept above 100%. The results also indicate that the reaction did not perform in the absence of $H_2O_2$ and very low yield was obtained (Table 1, entry 12). The effect of changing catalyst loaded (0.007, 0.009, 0.010 and 0.025 g) on methyl phenyl sulfide conversion was studied (Table 1, entries 13–15 and 5), and it indicates that the existence of catalyst is vital for this reaction. The highest yield was obtained in the presence of 0.025 g $CoFe_2O_4$-DAN-Cu(II) nanocatalyst. It is shown that no detectable product was observed when the reaction was carried out in the absence of the $CoFe_2O_4$-DAN-Cu(II) catalyst (Table 1, entry 6). It should be mentioned that only 40% was obtained in the presence of $CuCl_2 \cdot 2H_2O$ used as a catalyst (Table 1, entry 16). As shown, using ethanol as the solvent in the presence of catalytic amounts of $CoFe_2O_4$-DAN-Cu(II) (0.025 g) and $H_2O_2$ (0.5 mL) at 25 °C was realized to be the optimized conditions (Table 1, entry 5).

Because of the successful oxidation of methyl phenyl sulfide, the reactions of different sulfides under optimized conditions were examined (Table 2). Sulfoxides were prepared at excellent conversion in a short reaction time. It can be seen that phenyl sulfide with an electron-withdrawing group showed a longer

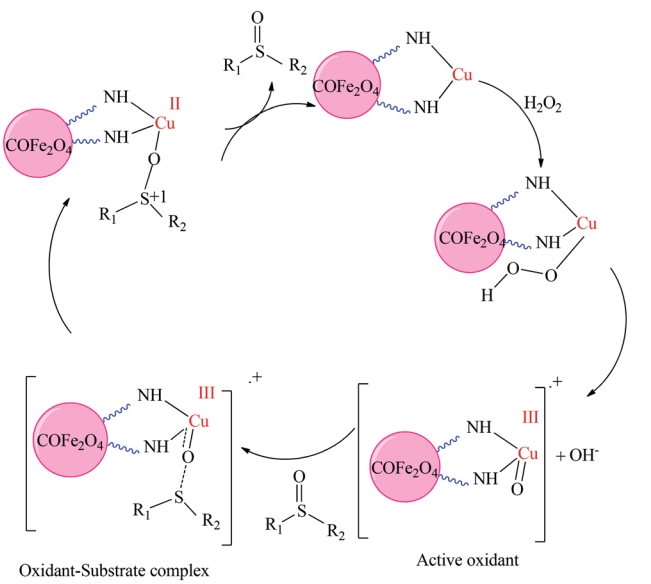


Scheme 2 Proposed mechanism for the oxidation of sulfides in the presence of $CoFe_2O_4$-DAN-Cu(II).

reaction time and a lower yield (Table 2, entries 8 and 9). Researches show that in this case, the resonance of the sulfur electron pair with the aromatic ring is effective. Moreover, alkyl sulfides with longer alkyl chains proceeded in higher reaction times (Table 2, entries 4 and 6). These results are probably due to the substrate's insolubility in ethanol that decreased the substrate concentration in the reaction mixture and lowered the reaction rate. The selectivity of the catalyst is highly important in the industry and in the mentioned reaction, oxidation of sulfides with the optimal conditions is thoroughly selective and the sulfone was not observed as a by-product.

Sulfoxide usually acts as an electrophile, while sulfide is a nucleophilic reductant. This dual performance of the sulfur atom in the sulfide and the sulfoxide makes it an appropriate system to investigate nucleophilic behavior *versus* oxidant electrophilic behavior. $H_2O_2$ as a mild oxidizing agent reacts slowly and must be activated by homogeneous or heterogeneous catalysts. The catalytic cycle for the oxidation of sulfide by $H_2O_2$ catalyzed by the $CoFe_2O_4$-DAN-Cu(II) catalyst is proposed in Scheme 2. The explanation for this transformation is the formation of the intermediate **A** using the reaction of $CoFe_2O_4$-DAN-Cu(II) with $H_2O_2$, followed by the conversion of the intermediate **A** to the active oxidant. Then, nucleophile sulfide attacks active oxidants and with heterolytic cleavage of the Cu–O bond yields sulfoxide.[56,57]

In continuation of our experiment, the catalytic activity of $CoFe_2O_4$-DAN-Cu(II) was examined for the synthesis of symmetrical sulfides. The effect of catalyst dosage, the nature of the solvents and bases, and the reaction temperature were optimized (Table 3). Initially, the reaction of the coupling of iodobenzene (1 mmol), thiourea (1 mmol) as a sulfur source and NaOH was chosen for a model reaction. In order to investigate the influence of the solvents, we utilized DMF, toluene, water, DMSO and PEG as solvents (Table 3, entries 1–5). As shown, the

Table 4 Synthesis of symmetrical sulfides in the presence of $CoFe_2O_4$-DAN-Cu(II) nanocatalysts[a]

| Entry | Substrate | Product | Time (h) | Yield[b] (%) | MP (°C) |
|---|---|---|---|---|---|
| 1 |  | 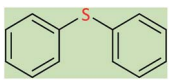 | 2.5 | 95 | Oil[55] |
| 2 | 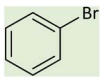 | 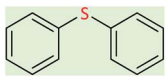 | 4 | 88 | Oil[55] |
| 3 |  | 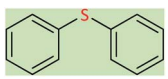 | 8 | 40 | Oil[58] |
| 4 | 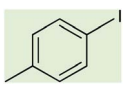 | 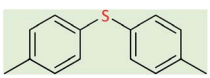 | 7 | 69 | Oil[58] |
| 5 | 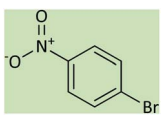 | 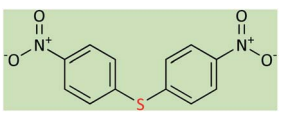 | 5.5 | 75 | 158–160 (ref. 56) |
| 6 | 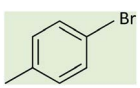 | 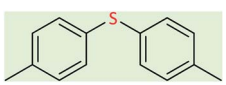 | 8 | 58 | Oil[58] |
| 7 | 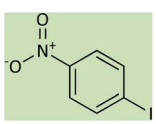 | 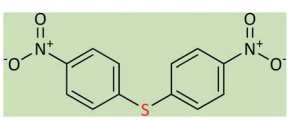 | 5 | 75 | 157–160 (ref. 58) |
| 8 | 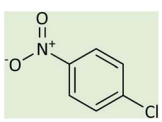 | 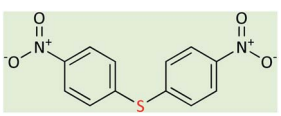 | 9.5 | 45 | 158–160 (ref. 59) |
| 9 | 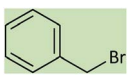 | 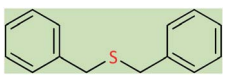 | 4.5 | 78 | 44–46 (ref. 56) |
| 10 | 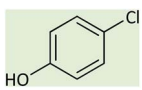 | 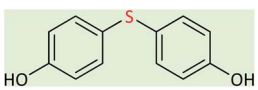 | 10.5 | 43 | 150–153 (ref. 26) |

[a] Reaction conditions: catalyst (0.030 g), aryl halide (1 mmol), $CH_4N_2S$ (1 mmol), base (0.040 g) and solvent (3 mL) at 130 °C. [b] Isolated yields.

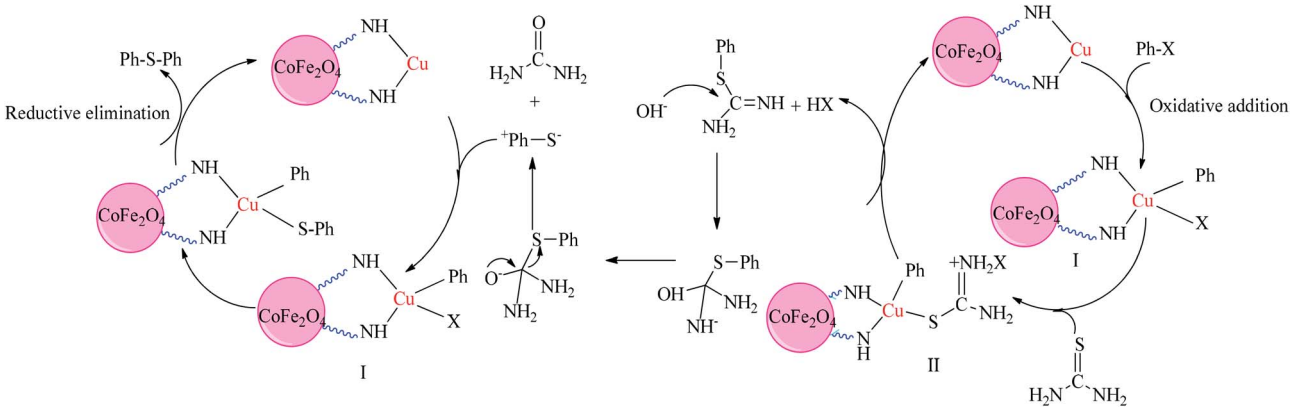


Scheme 3 Plausible mechanism for the symmetrical sulfide synthesis by $CoFe_2O_4$-DAN-Cu(II) nanocatalysts.

reaction did not proceed in PEG, $H_2O$ and yielded only 35% in toluene (Table 3, entries 1, 2 and 5). The sulfide synthesis reaction was accomplished in excellent yields in DMSO as the reaction solvent (Table 3, entry 4), whereas the product yield prepared in DMF under the same condition was 52% (Table 3, entry 3). Additionally, different bases for the sulfide synthesis were checked (Table 3, entries 16, 17 and 4), and 0.4 g of NaOH was found to be the desired amount of the base (Table 3, entry 4). The reaction was carried out for catalytic amounts of thiourea (Table 3, entries 7, 8 and 4). The highest yield of diphenyl sulfide was achieved using 1 mmol of thiourea without increasing the catalyst loading (Table 3, entry 4). In order to gain the best reaction temperature, the mentioned reaction was investigated at several temperatures (Table 3, entries 12–15 and 4), and the results indicate that increasing temperature from 45 to 130 °C increased the yield. Therefore, the optimized temperature was found to be 130 °C. The effect of the catalyst amount was also checked (Table 3, entries 9–11 and 4), and the results show that with the increase in the amount of catalyst from 0.008 to 0.05, the yield also increased from 37% to 95%. The control experiment showed that catalyst-free conditions yielded trace amounts of products even after 5 hours (Table 3, entry 6). Furthermore, the reaction was carried out in the presence of $CuCl_2 \cdot 2H_2O$ as the catalyst, which afforded diphenyl sulfide in low yields (Table 3, entry 18).

Several derivatives of aryl halides with electron-donating and electron-withdrawing groups were examined under optimal conditions (Table 4). In the synthesis of symmetrical sulfides, used haloarenes follow ArI > ArBr > ArCl (Table 4, entries 1–3). Aromatic haloarenes with electron-withdrawing groups are more reactive in comparison to electron-donating groups (Table 4, entries 4 and 7). Selectivity is one of the most notable advantages of this system by which the coupling reaction of 1-bromo-4-nitrobenzene, 1-chloro-4-nitrobenzene, and 1-iodo-4-

Table 5 Optimization of conditions for oxidative coupling of thiols in the presence of $CoFe_2O_4$-DAN-Cu(II)

| Entry | Catalyst (mg) | Oxidation agent | Solvent | Temp. (°C) | Time (min) | Yield[a] (%) |
|---|---|---|---|---|---|---|
| 1 | 25 | $H_2O_2$ (0.4 mL) | Acetonitrile | 25 | 35 | 85 |
| 2 | 25 | $H_2O_2$ (0.4 mL) | *n*-Hexane | 25 | 180 | 25 |
| 3 | 25 | $H_2O_2$ (0.4 mL) | $CH_2Cl_2$ | 25 | 40 | 60 |
| 4 | 25 | $H_2O_2$ (0.4 mL) | EtOAc | 25 | 35 | 87 |
| 5 | 25 | $H_2O_2$ (0.4 mL) | $H_2O$ | 25 | 30 | 75 |
| 6 | 25 | $H_2O_2$ (0.4 mL) | Ethanol | 25 | 20 | 96 |
| 7 | — | $H_2O_2$ (0.4 mL) | Ethanol | 25 | 140 | Trace |
| 8 | 25 | $H_2O_2$ (0.45 mL) | Ethanol | 25 | 25 | 97 |
| 9 | 25 | $H_2O_2$ (0.3 mL) | Ethanol | 25 | 40 | 80 |
| 10 | 25 | $H_2O_2$ (0.2 mL) | Ethanol | 25 | 40 | 75 |
| 11 | 25 | $H_2O_2$ (0.1 mL) | Ethanol | 25 | 40 | 65 |
| 12 | 25 | — | Ethanol | 25 | 140 | Trace |
| 13 | 8 | $H_2O_2$ (0.4 mL) | Ethanol | 25 | 40 | 58 |
| 14 | 10 | $H_2O_2$ (0.4 mL) | Ethanol | 25 | 40 | 72 |
| 15 | 20 | $H_2O_2$ (0.4 mL) | Ethanol | 25 | 25 | 86 |
| 16 | $CuCl_2 \cdot 2H_2O$ | $H_2O_2$ (0.4 mL) | Ethanol | 25 | 75 | 45 |
| 17 | 25 | $NaClO_2$ (1 mmol, 0.090 g) | Methanol | 5 | 20 | 93 |
| 18 | 25 | $NaIO_4$ (1 mmol, 0.213 g) | $H_2O$ | 25 | 25 | 100 |
| 19 | 25 | DBDMH (0.2 eq.) | $CHCl_3$ | 25 | 2 | 96 |

[a] Isolated yields.

Table 6 Synthesis of disulfides in the presence of $CoFe_2O_4$-DAN-Cu(II) nanocatalysts[a]

| Entry | Substrate | Product | Time (min) | Yield[b] (%) | MP (°C) |
|---|---|---|---|---|---|
| 1 | 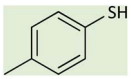 | 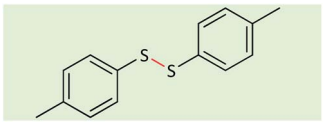 | 20 | 96 | 38–40 (ref. 26) |
| 2 | 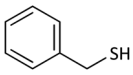 | 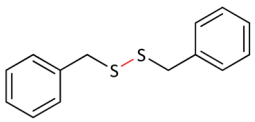 | 40 | 92 | 65–71 (ref. 55) |
| 3 | 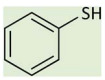 | 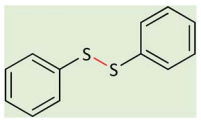 | 25 | 96 | 58–60 (ref. 53) |
| 4 | 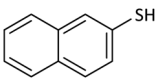 | 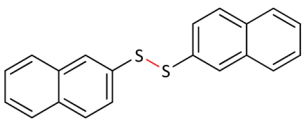 | 30 | 95 | 134–136 (ref. 26) |
| 5 | 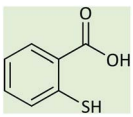 | 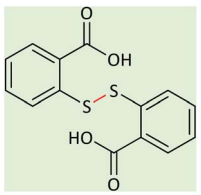 | 45 | 88 | 276–278 (ref. 26) |
| 6 | 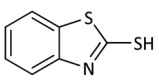 | 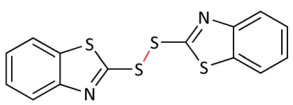 | 20 | 90 | Oil[55] |
| 7 | 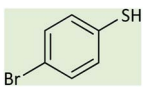 | 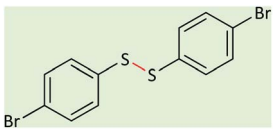 | 60 | 86 | 88–90 (ref. 26) |
| 8 | 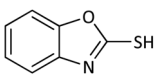 | 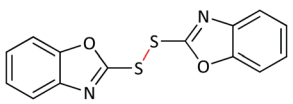 | 65 | 90 | 98–99 (ref. 55) |
| 9 | 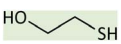 | 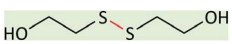 | 35 | 95 | Oil[26] |
| 10 | 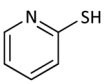 | 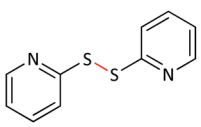 | 35 | 90 | 55–57 (ref. 55) |

[a] Reaction conditions: catalyst (0.025 g), thiol (1 mmol), 30% $H_2O_2$ (0.4 mL) and solvent (3 mL) at 25 °C. [b] Isolated yields.

nitrobenzene resulted in the favorite product without extra changes.

A plausible mechanism for this transformation is outlined in the presence of the $CoFe_2O_4$-DAN-Cu(II) nanocatalyst (Scheme 3). First, the oxidative addition of Cu nanoparticles to the aryl halide forms intermediate (**I**). Then, the coupling reaction of the aryl halide with thiourea generates intermediate (**II**), which is transmitted to a thiol anion in the presence of NaOH. Finally, thiol anion reacts with intermediate (**I**) to produce the sulfide product as well as the initial catalyst.[60]

At last, the $CoFe_2O_4$-DAN-Cu(II) catalytic system was examined for oxidative coupling of thiols to disulfides using 4-methylthiophenol as the model substrate. To find out the optimized reaction conditions, the presence of various catalytic amounts of $CoFe_2O_4$-DAN-Cu(II) and several organic solvents using different amounts of $H_2O_2$ was tested (Table 5). Initially, the model reaction was carried out in several solvents such as acetonitrile, *n*-hexane, EtOAc, $CH_2Cl_2$, EtOH and $H_2O$. Among them, acetonitrile (85%), EtOAc (87%) and EtOH (96%) showed better conversion for selective disulfide synthesis. However,

because of the nontoxic and availability properties, EtOH was chosen as a green solvent (Table 5, entries 1–6). In order to study the effect of the oxidant nature, the reaction was also investigated in the presence of several oxidants such as $NaClO_2$, $NaIO_4$ and 1,3-dibromo-5,5-dimethyl-hydantoin (DBDMH) instead of $H_2O_2$ (Table 5, entries 17–19). Compared with the other oxidants, $H_2O_2$ showed higher activity. Then, the effect of the catalyst amount (0.008, 0.010, 0.020 and 0.025 g) on 4-methylthiophenol conversion was studied, and it was observed that the activity of the catalyst was affected by the amount of the catalyst (Table 5, entries 13–15 and 6). The highest yield was obtained in the presence of 0.025 g of $CoFe_2O_4$-DAN-Cu(II). The blank reaction showed that catalyst-free conditions produced trace amounts of products even after 140 minutes (Table 5, entry 7). When the catalyst $CoFe_2O_4$-DAN-Cu(II) was replaced with $CuCl_2 \cdot 2H_2O$, the desired oxidation product was obtained in lower yields (45%) (Table 5, entry 16).

Utilizing the optimum reaction condition, a variety of substituted thiols were selected for the synthesis of disulfides (Table 6). The results indicate that the $CoFe_2O_4$-DAN-Cu(II) nanocatalyst exhibited efficient catalytic activity with good to high yields in the reaction time. It was observed that aliphatic thiols oxidized more slowly than aromatic ones (Table 6, entries 1 and 9). It is also shown that aromatic thiols including electron-donating groups are more reactive than thiols with electron-withdrawing groups (Table 6, entries 1 and 7). This system shows good chemoselectivity by which the hydroxyl group of 2-mercaptoethanol remains constant, and a thiol functional group of these molecules was oxidized to disulfide. Furthermore, selectivity is one of the main important features of this system. Because of the selectivity of the mentioned heterogeneous catalyst, there is no overoxidation to thiosulfinates, disulfoxides, sulfinyl sulfones, or disulfones.

A plausible mechanism for this transformation is shown in Scheme 4, on the basis of the literature works.[23] A comparison for the efficiency of the catalytic activity of $CoFe_2O_4$-DAN-Cu(II) for the oxidation of sulfides to sulfoxides (Table 7, entries 1–7), synthesis of symmetrical sulfides (Table 7, entries 8–11), and oxidative coupling of thiols to disulfides (Table 7, entries 12–15) with several previously reported methods is presented. Recently, the use of $Co@SiO_2[(EtO)_3Si–L_3]/Mn(III)$ (Table 7, entry 1), $FeNi_3/SiO_2$ (Table 7, entry 3), Mn(III)-binapthyl Schiff base diamine-SBA-15 (Table 7, entry 4), $K_6H_8[(SeV_{10}O_{28}(SeO_3)_3)_2(M(H_2O)_4)] \cdot 24H_2O$ (Table 7, entry 5), VO-TAPT-2,3-DHTA COF (Table 7, entry 6), $CuFe_2O_4$ (Table 7, entry 12), Pd-isatin Schiff base@KIT-6 (Table 7, entry 13), and $TiO(O_2CCF_3)$/NaI/thiol (Table 7, entry 14) was reported for oxidation reactions. These methods need toxic organic solvents with high reaction times. The use of Mn(III)-binapthyl Schiff base diamine-SBA-15 (Table 7, entry 4), $K_6H_8[(SeV_{10}O_{28}(SeO_3)_3)_2(M(H_2O)_4)] \cdot 24H_2O$ (Table 7, entry 5), VO-TAPT-2,3-DHTA COF (Table 7, entry 6), and Pd-isatin Schiff base@KIT-6 (Table 7, entry 13) as the catalyst for oxidation reactions was reported, requiring high reaction times. Moreover, harsh conditions are found when using $TiCl_3(O_3SCF_3)$ (Table 7, entry 14), $TiO(O_2CCF_3)_2$ (Table 7, entry 14), $CuFe_2O_4$ (Table 7, entry 12), and ethyl 2-oxocyclohexanecarboxylate as catalysts (Table 7, entry 8) in oxidation reactions and sulfide synthesis, respectively. $FeNi_3/SiO_2$ (Table 7, entry 3) causes to use of *m*-CPBA instead of green oxidant $H_2O_2$. Accordingly, this catalyst affords an absolutely green procedure, and these results clearly accentuate the efficiency of this applied methodology.

### 3.3 Catalyst recycling

Recycling as one of the main important properties of nanomagnetic catalysts was also investigated by the synthesis of methyl phenyl sulfoxide, diphenyl sulphide, and 1,2-di-*p*-tolyldisulfane under optimized conditions. After completion of the reactions, the $CoFe_2O_4$-DAN-Cu(II) nanocatalyst was removed from the reaction mixture by a magnet and used in the next cycle under mentioned optimum conditions. As shown in Fig. 4, the catalyst can be recycled for nine runs without any considerable loss of catalytic activity.

In order to clarify the changes in the chemical structure of the prepared catalyst towards oxidation during the nine cycles, FE-SEM and FT-IR analyses were performed. SEM and FT-IR analyses of this catalyst after nine runs show no significant changes during the reaction time (Fig. 5). Moreover, the amount of copper on recovered $CoFe_2O_4$-DAN-Cu(II) was measured by ICP-OES analysis for the conversion of methyl phenyl sulfide to methyl phenyl sulfoxide in the fresh catalyst and after nine consecutive cycles, it was found to be 0.43 mmol $g^{-1}$ and 0.32 mmol $g^{-1}$, which indicates the minimum amount of Cu leaching in the catalytic process. Furthermore, AAS analysis of the reaction mixture after catalyst removal showed no considerable amount of copper. AAS analyses of the recycled $CoFe_2O_4$-DAN-Cu(II) catalyst also exhibited no significant (<0.001 mmol $g^{-1}$ of Cu) differences compared with the fresh catalyst, presenting that no considerable copper leaching occurred during the catalytic processes. Moreover, regarding the heterogeneous nature of $CoFe_2O_4$-DAN-Cu(II), the oxidation of methyl phenyl sulfide has been examined by a hot filtration experiment under optimal reaction conditions. In this test, we found the yield of

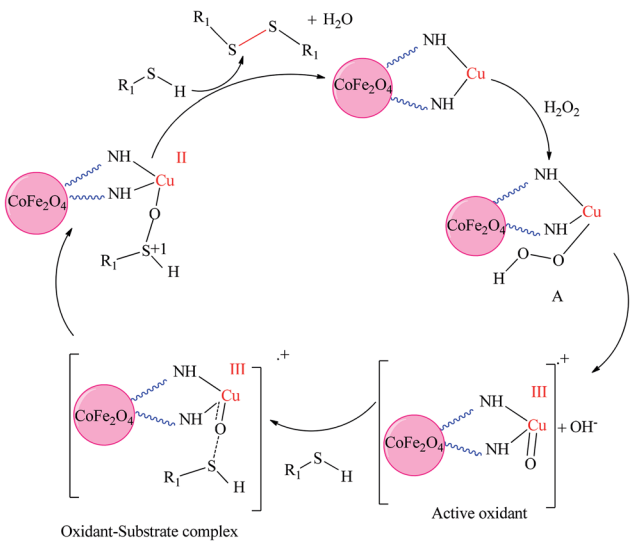


Scheme 4 Plausible mechanism for the oxidative coupling of thiols by $CoFe_2O_4$-DAN-Cu(II) nanocatalysts.

Table 7 Comparison of $CoFe_2O_4$-DAN-Cu(II) in the catalytic oxidation reactions and synthesis of sulfide derivatives with other catalysts[a]

| Entry | Substrate | Catalyst | Time (min) | Catalyst loading | Condition | Yield[b] (%) | Ref. |
|---|---|---|---|---|---|---|---|
| 1 | [1]Ph–S–$CH_3$ | $Co@SiO_2[(EtO)_3Si–L_3]$/ Mn(III) | 50 | 0.06 g | Methyl phenyl sulfide (0.5 mmol), acetonitrile, 90 μL $H_2O_2$ and 65 °C | 99 | 61 |
| 2 | [2]Ph–S–$CH_3$ | MNP@TA-IL/W | 60 | 0.4 mol% | $H_2O$, 1.5 mmol $H_2O_2$ and 25 °C | 99 | 62 |
| 3 | [3]Ph–S–$CH_3$ | $FeNi_3/SiO_2$ | 60 | 0.04 | DCM (2.0 mL), *m*-CPBA (2.0 mmol) and r.t | 99 | 63 |
| 4 | [4]Ph–S–$CH_3$ | Mn(III)-binapthyl Schiff base diamine-SBA-15 | 300 | 50 mg | $CH_2Cl_2$ and 25 °C | 94 | 64 |
| 5 | [5]Ph–S–$CH_3$ | $M^{2+}$-sandwiched POVs: $K_6H_8[(SeV_{10}O_{28}(SeO_3)3)_2(M(H_2O)_4)]\cdot 24H_2O$ | 60 | 2 μmol | $CH_3OH$ and 25 °C | 97.9 | 65 |
| 6 | [6]Ph–S–$CH_3$ | VO-TAPT-2,3-DHTA COF | 240 | 20 mg | $CH_3CN$ and 25 °C | 95 | 66 |
| 7 | Ph–S–$CH_3$ | $CoFe_2O_4$-DAN-Cu(II) | 15 | 0.025 g | $C_2H_5OH$ and 25 °C | 99 | **This work** |
| 8 | [8]Iodobenzene | Ethyl 2-oxocyclohexanecarboxylate | 1200 | 0.1 mmol | 80 °C and under Ar | 96 | 67 |
| 9 | [9]Iodobenzene | $Fe_3O_4$@SBTU@Ni(II) | 210 | 0.030 | DMSO and 130 °C | 94 | 60 |
| 10 | [10]Iodobenzene | MNP-Si-NHC(Pyr)-Ni | 600 | 10 mol% | DMF, 100 °C, base (2 mmol) and thiol (1 mmol) | 92 | 68 |
| 11 | Iodobenzene | $CoFe_2O_4$-DAN-Cu(II) | 150 | 0.030 g | DMSO and 130 °C | 95 | **This work** |
| 12 | [12]Thiophenol | $CuFe_2O_4$ | 24 h | 10 mol% | 1.80 mmol of halide, 2.0 eq. of base, 5 mL of 1,4-dioxane and under $N_2$ atmosphere | 95 | 69 |
| 13 | [13]4-Methyl thiophenol | Pd-isatin Schiff base@KIT-6 | 30 | 0.025 g | $CH_3CN$, 25 °C and 5 mmol $H_2O_2$ | 95 | 70 |
| 14 | [14]Thiophenol | $TiO(O_2CCF_3)_2$/NaI/thiol | 150 | 1 mmol | $CH_3CN$ and under reflux conditions | 100 | 71 |
| 15 | Thiophenol | $CoFe_2O_4$-DAN-Cu(II) | 20 | 0.025 g | $C_2H_5OH$ and 25 °C | 96 | **This work** |

[a] Abbreviations: [1]Schiff-base Mn(III) and Co(II) complexes coated on Co nanoparticles, [2]tungstate ions loaded onto triazine-based ionic liquid-functionalized magnetic nanoparticle, [3]$FeNi_3$ nanoparticle conjugated tetraethyl orthosilicate; [4]chloro(*S*,*S*)(−)[*N*-3-*tert*-butyl-5-chloromethylsalicylidene]-*N*′-[3′,5′-ditert-butylsalicylidene]1,1′-binapthyl-2,2′-diamine manganese(III) complex over modified surface of SBA-15, [5]transition metal-sandwiched heteropolyoxovanadate complexes, [6]complex vanadium of Schiff base of 2,4,6-tris(4-aminophenyl)-1,3,5-triazine–2,3-dihydroxyterephthaldehyde (TAPT–2,3-DHTA), [8]ethyl 2-oxocyclohexanecarboxylate ligand in the presence of $Cu_2O$ as catalyst, [9]nickel(II) complex supported on modified surface of $Fe_3O_4$. [10]Magnetite/silica nanoparticles supported N-heterocyclic carbene nickel catalyst, [12]copper ferrite nanoparticles, [13]Pd(II)-isatin Schiff base complex immobilized into three-dimensional mesoporous silica KIT-6, [14]$TiCl_3(O_3SCF_3)$ and $TiO(O_2CCF_3)_2$ as the catalyst. [b] Isolated yields.

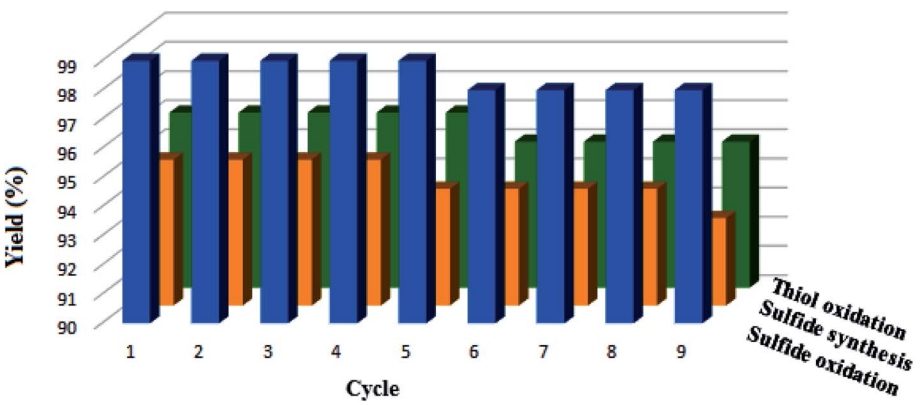


Fig. 4 Reusability of the $CoFe_2O_4$-DAN-Cu(II) nanocatalyst in the sulfide oxidation, sulfide synthesis and oxidative coupling of thiols.

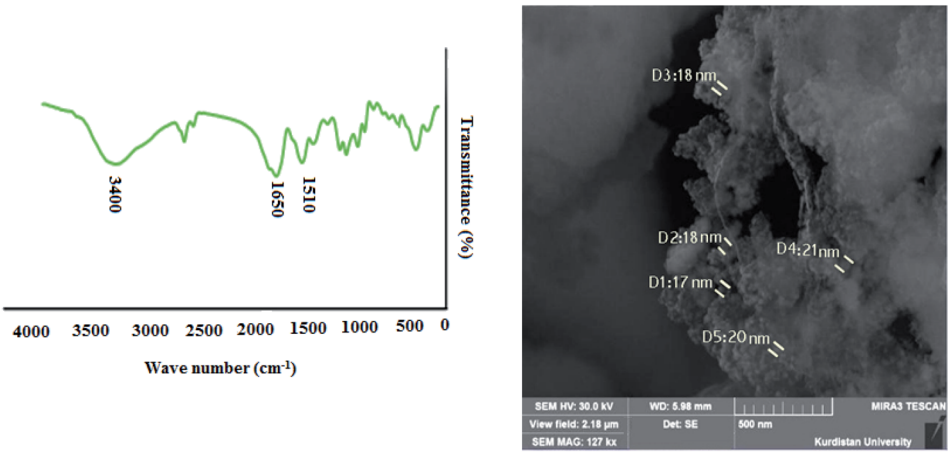


Fig. 5 FT-IR and SEM analyses of the $CoFe_2O_4$-DAN-Cu(II) nanocatalyst after nine runs.

product in a half time of the reaction to be 65%. Then, the reaction was repeated and at half time of the reaction, the catalyst was separated using a magnet and allowed to react further. The yield of the reaction in this stage was 69%, which confirmed that the reaction proceeded heterogeneously and after hot filtration, the reaction of the residual mixture was completely stopped.

### 3.4 Catalyst poisoning test

Another heterogeneity test was performed with Hg poisoning. Hg(0) can poison catalysts, either by amalgamating the applied metal or adsorbing on the metal surface.[72] The sulfide oxidation was conducted under the same mentioned conditions, except the addition of elemental Hg (1 mmol) to the reaction mixture at 50% conversion of methyl phenyl sulfide to methyl phenyl sulfoxide. No product was gained with this procedure, which is strong evidence that the catalyst nature is heterogeneous.

## 4. Conclusion

An efficient $CoFe_2O_4$-DAN-Cu(II) nanocatalyst has been successfully synthesized using an anchored Cu complex on the stable and bidentate ligand 1,8-diaminonaphthalene-modified $CoFe_2O_4$ nanoparticles. Then, the prepared nanostructure has been characterized by techniques such as SEM, EDX, ICP-OES, TGA, XRD, VSM, FT-IR and TEM. The immobilized Cu complex exhibits remarkable catalytic activity in the oxidation of sulfides and thiols in a green catalytic system ($C_2H_5OH$ as a solvent and $H_2O_2$ as an oxidant). All studied sulfides and thiols were oxidized to their corresponding sulfoxides and disulfides without production of any by-product. Moreover, the C–S cross-coupling reaction produced in the clean suspension of a variety of diarylsulfides appropriate to good yields. This system has many benefits such as high yields, chemical stability and ease of catalyst separation using an external magnet. The nanocatalyst can be recycled and reused for next runs without any significant change in its catalytic activity.

## Conflicts of interest

There are no conflicts to declare.

## Acknowledgements

The authors wish to thank the financial support from the University of Kurdistan.

## Notes and references

1 M. Kazemi, M. Ghobadi and A. Mirzaie, *Nanotechnol. Rev.*, 2017, **7**, 43–93.
2 M. Kaushik and A. Moores, *Curr. Opin. Green Sustain. Chem.*, 2017, **7**, 39–45.
3 L. Zhou, C. Gao and W. Xu, *Langmuir*, 2010, **26**, 11217–11225.
4 S. R. Chaurasia, A. R. Tiwari and B. M. Bhanage, *J. Mol. Catal.*, 2019, **478**, DOI: 10.1016/j.mcat.2019.110565.
5 M. Bagherzadeh, M. Bahjati and A. Mortazavi-Manesh, *J. Organomet. Chem.*, 2019, **897**, 200–206.
6 A. R. Hajipour, D. M. Hosini and F. Mohammadsaleh, *New J. Chem.*, 2016, **40**, 6939–6945.
7 P. D. Stevens, G. Li, J. Fan, M. Yen and Y. Gao, *Chem. Commun.*, 2005, **35**, 4435–4437.
8 M. N. Chen, L. P. Mo, Z. S. Cui and Z. H. Zhang, *Curr. Opin. Green Sustain. Chem.*, 2019, **15**, 27–37.
9 R. S. Varma, *ACS Sustainable Chem. Eng.*, 2016, **4**, 5866–5878.
10 L. L. Chng, N. Erathodiyil and J. Y. Ying, *Acc. Chem. Res.*, 2013, **46**, 1825–1837.
11 S. Molaei, T. Tamoradi, M. Ghadermazi and A. Ghorbani-Choghamarani, *Microporous Mesoporous Mater.*, 2018, **272**, 241–250.
12 S. Lotfi, A. Nikseresht and N. Rahimi, *Polyhedron*, 2019, **173**, 114148.
13 C. Zhang, C. Li, J. Bai and H. Li, *Catal. Lett.*, 2015, **145**, 1764–1770.
14 F. Yakuphanoglu and M. Sekerci, *J. Mol. Struct.*, 2005, **751**, 200–203.

15 M. A. R. Da Silva, A. I. L. Ferreira, A. F. L. Santos, C. M. Ferreira, D. C. Barros, J. A. Reis, J. C. Costa, M. M. G. Calvinho, S. I. Rocha, S. P. Pinto and S. S. Freire, *J. Chem. Thermodyn.*, 2010, **42**, 371–379.
16 A. A. Aly and K. M. El-Shaieb, *Tetrahedron*, 2004, **60**, 3797–3802.
17 J. D. De León, S. Loera-Serna, T. A. Zepeda, D. Domínguez, B. Pawelec, A. M. Venezia and S. Fuentes-Moyado, *Fuel*, 2020, **266**, 117031.
18 E. Lagerspets, K. Lagerblom, E. Heliövaara, O. M. Hiltunen, K. Moslova, M. Nieger and T. Repo, *J. Mol. Catal.*, 2019, **468**, 75–79.
19 K. Patel, S. Kapoor, D. P. Dave and T. Mukherjee, *J. Chem. Sci.*, 2005, **117**, 311–316.
20 J. Guo, C. Lin, C. Jiang and P. Zhang, *Appl. Surf. Sci.*, 2019, **475**, 237–255.
21 P. Singh, N. Mahadevaiah, S. K. Parida and M. S. Hegde, *J. Chem. Sci.*, 2011, **123**, 577–592.
22 Y. Chen, B. He, A. Qin and B. Z. Tang, *Sci. China: Chem.*, 2019, **62**, 1017–1022.
23 S. T. Aziz and R. U. Islam, *Catal. Lett.*, 2018, **148**, 205–213.
24 M. Ghavami, M. Koohi and M. Z. Kassaee, *J. Chem. Sci.*, 2013, **125**, 1347–1357.
25 M. B. Gawande, A. Goswami, F. X. Felpin, T. Asefa, X. Huang, R. Silva, X. Zou, R. Zboril and R. S. Varma, *Chem. Rev.*, 2016, **116**, 3722–3811.
26 T. Tamoradi, N. Moeini, M. Ghadermazi and A. Ghorbani-Choghamarani, *Polyhedron*, 2018, **153**, 104–109.
27 S. Zolfagharinia, E. Kolvari, N. Koukabi and M. M. Hosseini, *J. Chem. Sci.*, 2017, **129**, 1411–1421.
28 A. Ghorbani-Choghamarani, Z. Darvishnejad and B. Tahmasbi, *Inorg. Chim. Acta*, 2015, **435**, 223–231.
29 Q. Liu, X. Zhao, F. Xu and G. Li, *Tetrahedron Lett.*, 2020, **61**, 151492.
30 Y. Dou, X. Huang, H. Wang, L. Yang, H. Li, B. Yuan and G. Yang, *Green Chem.*, 2017, **19**, 2491–2495.
31 H. Zhang, M. Zhou, L. Xiong, Z. He, T. Wang, Y. Xu and K. Huang, *Microporous Mesoporous Mater.*, 2018, **255**, 103–109.
32 N. Noori, M. Nikoorazm and A. Ghorbani-Choghamarani, *Microporous Mesoporous Mater.*, 2016, **234**, 166–175.
33 T. Tamoradi, M. Ghadermazi and A. Ghorbani-Choghamarani, *Catal. Lett.*, 2019, **149**, 2645–2646.
34 Z. Chen, C. Wu, Z. Zhang, W. Wu, X. Wang and Z. Yu, *Chin. Chem. Lett.*, 2018, **29**, 1601–1608.
35 M. Bagherzadeh, M. Hosseini and A. Mortazavi-Manesh, *Inorg. Chem. Commun.*, 2019, **107**, 107495.
36 M. G. Kermanshah and K. Bahrami, *RSC Adv.*, 2019, **9**, 36103–36112.
37 J. Tang, P. Yao, L. Wang, H. Bian, M. Luo and F. Huang, *RSC Adv.*, 2018, **8**, 40720–40730.
38 R. Hasanpour, F. Feizpour, M. Jafarpour and A. Rezaeifard, *New J. Chem.*, 2018, **42**, 7383–7391.
39 Y. Zhou, B. Xue, C. Wu, S. Chen, H. Liu, T. Jiu, Z. Li and Y. Zhao, *Chem. Commun.*, 2019, **55**, 13570–13573.
40 R. H. Wu, M. Guo, M. X. Yu and L. G. Zhu, *Dalton Trans.*, 2017, **46**, 14348–14355.
41 G. Saikia, K. Ahmed, C. Rajkhowa, M. Sharma, H. Talukdar and N. S. Islam, *New J. Chem.*, 2019, **43**, 17251–17266.
42 R. Limvorapitux, H. Chen, M. L. Mendonca, M. Liu, R. Q. Snurr and S. T. Nguyen, *Catal. Sci. Technol.*, 2019, **9**, 327–335.
43 M. Radko, A. Kowalczyk, P. Mikrut, S. Witkowski, W. Mozgawa, W. Macyk and L. Chmielarz, *RSC Adv.*, 2020, **10**, 4023–4031.
44 S. Hou, N. Chen, P. Zhang and S. Dai, *Green Chem.*, 2019, **21**(455), 1455–1460.
45 I. Malaescu, A. Lungu, C. N. Marin, P. Vlazan, P. Sfirloaga and G. M. Turi, *Ceram. Int.*, 2016, **42**, 16744–16748.
46 S. Golchinvafa, S. M. Masoudpanah and M. Jazirehpour, *J. Alloys Compd.*, 2019, **809**, 151746.
47 T. Tamoradi, A. Ghorbani-Choghamarani and M. Ghadermazi, *New J. Chem.*, 2017, **41**, 11714–11721.
48 D. Karthickraja, S. Karthi, G. A. Kumar, D. K. Sardar, G. C. Dannangoda, K. S. Martirosyan and E. K. Girija, *New J. Chem.*, 2019, **43**, 13584–13593.
49 B. L. Li, H. C. Hu, L. P. Mo and Z. H. Zhang, *RSC Adv.*, 2014, **4**, 12929–12943.
50 R. Mozafari and F. Heidarizadeh, *Polyhedron*, 2019, **162**, 263–276.
51 M. Nasrollahzadeh, Y. Bayat, D. Habibi and S. Moshaee, *Tetrahedron Lett.*, 2009, **50**, 4435–4438.
52 T. Tamoradi, M. Ghadermazi, A. Ghorbani-Choghamarani and S. Molaei, *Res. Chem. Intermed.*, 2018, **44**, 4259.
53 A. Ghorbani-Choghamarani, B. Tahmasbi, F. Arghand and S. Faryadi, *RSC Adv.*, 2015, **5**, 92174–92183.
54 T. Tamoradi, M. Ghadermazi and A. Ghorbani-Choghamarani, *Appl. Organomet. Chem.*, 2018, **32**, e3974, DOI: 10.1002/aoc.3974.
55 G. Azadi, Z. Taherinia, A. Naghipour and A. Ghorbani-Choghamarani, *J. Sulfur Chem.*, 2017, **38**, 303–313.
56 E. Rafiee, M. Joshaghani and P. Ghaderi-Shekhi Abadi, *J. Saudi Chem. Soc.*, 2017, **21**, 599–609.
57 A. M. Al-Ajlouni, T. M. Daiafla and M. El-Khateeb, *J. Mol. Catal. A: Chem.*, 2007, **275**, 139–147.
58 X. Ku, H. Huang, H. Jiang and H. Liu, *J. Comb. Chem.*, 2009, **11**, 338–340.
59 V. S. Pilyugin, S. L. Kuznetsova, Y. E. Sapozhnikov, G. E. Chikisheva, G. V. Kiseleva, T. P. Vorob'eva, E. V. Klimakova, N. A. Sapozhnikova, R. D. Davletov and Z. B. Galeeva, *Russ. J. Gen. Chem.*, 2008, **78**, 446–450.
60 A. Ghorbani-Choghamarani, Z. Moradi and G. Azadi, *J. Sulfur Chem.*, 2017, **39**, 237–251.
61 S. G. Saremi, H. Keypour, M. Noroozi and H. Veisi, *RSC Adv.*, 2018, **8**, 3889–3898.
62 S. H. Hosseini, M. Tavakolizadeh, N. Zohreh and R. Soleyman, *Appl. Organomet. Chem.*, 2018, **32**, e3953.
63 S. Ghiami, M. A. Nasseri, A. Allahresani and M. Kazemnejadi, *React. Kinet., Mech. Catal.*, 2019, **126**, 383–398.
64 P. Sharma and A. P. Singh, *Catal. Today*, 2012, **198**, 184–188.
65 J. Y. Niu, R. Wan, P. He, Z. Liu, X. Ma, P. Ma, V. Singh, C. Zhang, J. Niu and J. Wang, *Chem.–Eur. J.*, 2020, **26**, 8760–8766.

66 H. Vardhan, G. Verma, S. Ramani, A. Nafady, A. M. Al-Enizi, Y. Pan, Z. Yang, H. Yang and S. Ma, *ACS Appl. Mater. Interfaces*, 2018, **11**, 3070–3079.
67 H. J. Xu, X. Y. Zhao, J. Deng, Y. Fu and Y. S. Feng, *Tetrahedron Lett.*, 2009, **50**, 434–437.
68 H. J. Yoon, J. W. Choi, H. Kang, T. Kang, S. M. Lee, B. H. Jun and Y. S. Lee, *Synlett*, 2010, **16**, 2518–2522.
69 N. Panda, A. K. Jena and S. Mohapatra, *Appl. Catal., A*, 2012, **433**, 258–264.
70 S. Pakvojoud, M. Hatefi Ardakani, S. Saeednia and E. Heydari-Bafrooei, *J. Sulfur Chem.*, 2020, **41**, 561–580.
71 B. Zeynizadeh and N. Iranpoor, *J. Chin. Chem. Soc.*, 2003, **50**, 849–852.
72 A. Chatterjee and V. R. Jensen, *ACS Catal.*, 2017, **7**, 2543–2547.